Received: 30 November 2018 | Revised: 29 March 2019 | Accepted: 30 March 2019
DOI: 10.1002/aoc.4959

FULL PAPER

WILEY Applied Organometallic Chemistry

Phosphotungstic acid grafted zeolite imidazolate framework as an effective heterogeneous nanocatalyst for the one-pot solvent-free synthesis of 3,4-dihydropyrimidinones

Reza Tayebee[1,2]* | Mojtaba Fattahi Abdizadeh[3] | Nasrin Erfaninia[1] | Amirhassan Amiri[1] | Mehdi Baghayeri[1] | Roya Mohammadzadeh Kakhki[4] | Behrooz Maleki[1] | Effat Esmaili[2]

[1] Department of Chemistry, Hakim Sabzevari University, Sabzevar 96179-76487, Iran

[2] Department of Chemistry, Payame Noor University (PNU), Tehran 19395-4697, Iran

[3] Cellular and Molecular Research Center, Sabzevar University of Medical Sciences, Sabzevar, Iran

[4] Department of Chemistry, Faculty of Sciences, University of Gonabad, Gonabad, Iran

Correspondence
R. Tayebee, Department of Chemistry, Hakim Sabzevari, University, Sabzevar 96179-76487, Iran.
Email: rtayebee@hsu.ac.ir

M. Fattahi Abdizadeh, Cellular and Molecular Research Center, Sabzevar University of Medical Sciences, Sabzevar, Iran.
Email: fattahim@medsab.ac.ir

Phosphotungstic acid ($H_3PW_{12}O_{40}$, PTA) supported on ZIF-9(NH_2) was synthesized for the first time and performed as an effective and environmental friendly catalyst in the one-pot three component Biginelli condensation of different substituted benzaldehydes with ethyl acetoacetate and urea to afford the corresponding 3,4-dihydropyrimidin-2-(1H)-ones under solvent-free conditions. ZIF-9(NH_2) and the prepared nanocatalyst PTA@ZIF-9(NH_2) were characterized by XRD, FESEM, TEM, EDX, BET, AAS, TGA, UV–Vis, and FT-IR. After reaction, the nanocatalyst can be easily separated from the reaction mixture by centrifuge and the recovered catalyst can be reused for at least five times with a 14% reduction in yield after the fifth run. This study showed that ZIF-9(NH_2) can be utilized as a promising support for PTA and developed a highly active, stable and reusable heterogeneous catalyst under easy reaction condition in the multi-component organic synthesis.

KEYWORDS
3,4-Dihydropyrimidin-2-(1H)-ones, heterogeneous, MOF, PTA@ ZIF-9(NH_2), solvent free

1 | INTRODUCTION

Metal–organic frameworks (MOFs) consist of metallic nodes bonded by organic linkers, are currently received significant attention because of their versatile properties.[1–3] They have been extensively used in catalysis,[4,5] gas storage,[6] separation,[7] ion exchange[8] and in drug delivery.[9] Compared to various microporous and mesoporous inorganic materials, MOFs showed several advantages such as structural diversity, flexibility and geometrical control by functionalization with different organic linkers.[10,11]

Application of MOFs in catalysis is limited due to their inert microstructures; however, further investigations to assess application of these materials in catalysis may be interesting. Zeolite imidazolate frameworks (ZIFs), as a new subclass of MOFs, involve highly desirable properties of both zeolites and conventional MOFs and are recently considered as profound highly crystalline materials with adequate porosity and easy tunability of the pore size/shape catalysts or catalyst supports by several research groups.[12,13] ZIFs are extended three-dimensional structures constructed from tetrahedral metal atoms (e.g., Zn, Co, Cu) bridged by imidazolate linkers[12] producing nanosized pores formed by four, six, eight, and twelve

---

*Electronic supplementary information (ESI) available.

membered rings ZnN_4, CoN_4, or CuN_4 tetrahedral clusters.[13] A number of applications have been explored for ZIFs as catalysts or catalyst supports in hydrogenation,[14] esterification,[15] transesterification,[16] hydrogenolysis,[17] reduction reactions,[18] as sensors,[19] and in many organic transformations.[19–23] Among various ZIFs, the subgroup of ZIF-9 also showed interesting catalytic and photocatalytic activities in the hydrogen generation,[24] oxidation reactions,[25] separation purposes[26] and in organic synthesis.[27]

Since, unsupported heteropolyacids are very soluble in polar solvents and generally induce their catalytic activities under homogeneous conditions, different supports can be employed to build up super acidic heterogeneous catalysts applicable in polar organic solvents. Indeed, our previous efforts revealed that the catalytic activity and acidity of the supported heteropolyacids depend mainly on the loading and nature of the carrier. However, leaching of the supported heteropolyacid, as a main drawback, reflects low interaction of this strong bronsted acid with the support material.[28–32]

In this work, we wish to report direct grafting of highly dispersed phosphotungstic acid into the cage of ZIF-9(NH_2). Then, the prepared nanocatalyst PTA@ZIF-9(NH_2) was applied for the Biginelli condensation of different substituted benzaldehydes with ethyl acetoacetate and urea to achieve the corresponding 3,4-dihydropyrimidin-2-(1H)-ones (Scheme 1). Dihydropyrimidinones have received charismatic assessment due to their wide range of pharmacological and therapeutic properties, such as antiviral, anti-tumor, antibacterial and anti-inflammatory.[33–37] Although, a number of protocols have been introduced for the synthesis of 3,4-dihydropyrimidin-2(1H)-ones; however, considering operational drawbacks such as needing strongly acidic condition, high temperature, long reaction time, and stoichiometric amounts of expensive reagents necessitate the discovery of new synthetic methodologies.

2 | EXPERIMENTAL

2.1 | Materials and methods

Cobalt nitrate hexahydrate (99%), 2-aminobenzimidazole (98%) and phosphotungstic acid were purchased from Merck and used as received without further purification. All synthesized dihydropyrimidinones were characterized by comparison of their spectral and physical data with those reported in the literature.[38] Progress of the reactions was monitored by TLC. Infrared spectra were recorded on 8700 *Shimadzu* Fourier Transform spectrophotometer using KBr windows. ^1H and ^{13}C NMR spectra were recorded on a Bruker AVANCE 300-MHz instrument using TMS as internal reference. Data for ^1H NMR are reported as follows: chemical shift (δ) and multiplicity (s: singlet, d: doublet, t: triplet, q: quartet, m: multiplet, qt: quintuple, dq: doublet of quartets, br: broad). X-ray diffraction patterns were obtained on a STOE diffractometer with Cu Kα radiation. Electron microscopy was performed on a Phillips XL-30 scanning electron microscope (SEM). Transmission Electron Microscopy was studied by TEM-Philips EM 208S operating at 100 kV. The BET surface areas and pore size distributions were acquired from N_2 adsorption–desorption isotherms at 77 K on a Belsorp-mini II (BEL Japan, Inc.). Thermal stability analysis was performed with thermogravimetric analysis (TGA, Q600 TA). Melting points were recorded with a Bumstead electrothermal type 9200 melting point apparatus. Ultraviolet–visible spectra were obtained on a Photonix UV–Vis Array spectrophotometer, Model Ar 2015.

2.2 | Preparation of ZIF-9(NH_2)

Co $(bIm)_2\cdot(DMF)(H_2O)$ abbreviated ZIF-9(NH_2) was prepared according to the reported procedure by Yaghi with a slight modification.[39] A solid mixture of Co$(NO_3)_2\cdot 6H_2O$ (2.10 g, 7.21 mmol) and 2-aminobenzimidazole (0.690 g, 5.08 mmol) were dissolved in 180 ml of N, N′-dimethylformamide (DMF). Then, the mixture was transferred to a tightly capped Teflon vial and heated at a rate of 5 °Cmin^{-1} to 140 °C and held at this temperature for 48 hr. After removal of the mother liquor, chloroform (20 ml) was added to the vial. The obtained pale pink polyhedral crystals were collected from the upper layer, washed with DMF (10 ml × 3), and dried in air for 2 hr.

2.3 | Preparation of PTA@ZIF-9(NH_2) and studying grafting of PTA into ZIF-9(NH_2)

The wet impregnation of phosphotungstic acid into ZIF-9(NH_2) was performed by dissolving 25 mg of

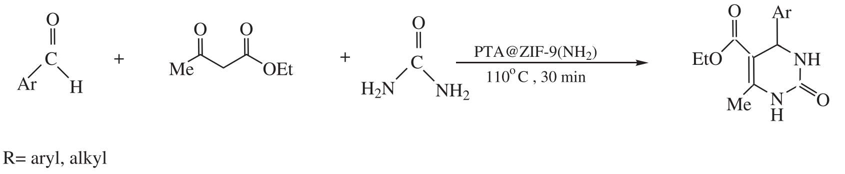

SCHEME 1 General scheme for the three component condensation of urea, aldehyde, and ethyl acetoacetate

phosphotungstic acid (PTA) in 40 ml methanol. Then, 50 mg of ZIF-9(NH_2) was added to the PTA solution and the mixture was refluxed for 4 hr. Thereafter, the solid was separated and washed with 4 × 8 ml of methanol to resolve the unreacted PTA from the surface of ZIF-9(NH_2). Finally, the purple crystals of PTA@ZIF-9(NH_2) were separated and dried at 70 °C for 15 hr (Scheme 2). Figure 1 displays UV–Vis spectral changes with time after addition of 0.5 g ZIF-9(NH_2) to 20 ml methanol solution of PTA (0.1 g) under reflux. This study showed that ~94% of PTA was grafted into ZIF-9(NH_2) after 2.5 hr and 18.8 wt% PTA@ZIF-9(NH_2) was attained. This finding was also confirmed by ICP based on the tungsten content. To ensure no significant leaching of PTA from ZIF-9(NH_2), a dried fresh sample of the impregnated PTA@ZIF-9(NH_2) was refluxed in methanol for 4 hr. Then, the solid catalyst was filtered and the filtrate was tested for existence of PTA by UV–Vis. A weak absorption band around 268 nm was developed; which confirmed small leaching of PTA into the methanol solution. To confirm PTA@ZIF-9(NH2) framework is stable even after 4 hr reflux in methanol, XRD of the target ZIF-9(NH_2) after reflux was compared with the newly prepared one (data are not shown). Very similar XRD diffractions proved that the ZIF structure was unchanged after 4 hr reflux in methanol.

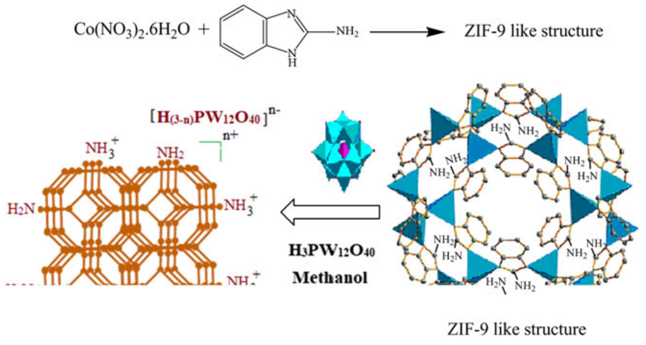

SCHEME 2 Schematic for the preparation of PTA@ZIF-9(NH_2) catalyst. A part of the schematic is reproduced with permission[23,64]

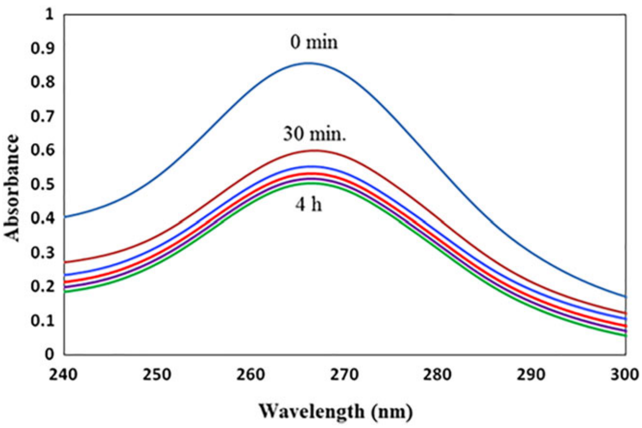

FIGURE 1 UV–Vis spectral changes during loading of PTA onto ZIF-9(NH_2)

2.4 | General procedure for the preparation of 3, 4-dihdropyrimidin-2(1H)-ones

A solution of aldehyde (1 mmol), ethyl acetoacetate (1.2 mmol), and urea (1.5 mmol) was heated to 110 °C under solvent-free condition in the presence of the desired amount of PTA@ZIF-9(NH_2) nanocatalyst. Completion of the reaction was monitored by TLC. After completion, the reaction mixture was cooled to room temperature, dissolved in minimum ethanol and filtered to separate the catalyst. Then, the crude product was poured into crushed ice with thorough stirring for 5 min. The desired dihydropyrimidinone was further purified by crystallization in ethanol. Spectral data of some selected compounds are obtained as the supporting material.

3 | RESULTS AND DISCUSSION

In this work, the ZIF-9(NH_2) was synthesized using cobalt (II) nitrate hexahydrate and 2-aminobenzimidazole by a solvothermal method in DMF. The ZIF-9(NH_2) was then characterized using different techniques as described below.

3.1 | Structural characterization of the hybrid nanomaterial

3.1.1 | FT-IR spectroscopy

FT-IR spectroscopy was carried out to confirm grafting of PTA into ZIF-9(NH_2) and formation of the final material PTA@ZIF-9(NH_2). FT-IR spectra of bare ZIF-9(NH_2) and PTA@ZIF-9(NH_2) are shown in Figure 2. A broad and strong band between 2400–3400 cm^{-1} is due to benzimidazole.[40,41] The band at 747 cm^{-1} in the spectral region is associated with the out-of-plane bending of imidazole ring, while peaks in the region of 900–1350 cm^{-1} are assigned to in-plane bending. The peaks at 1581–1645 and 3400 cm^{-1} would be due to the bending and stretching vibrations of N–H in imidazole ring, respectively. The intense band at 1456 cm^{-1} is associated with the entire ring stretching. FT-IR spectrum of PTA@ZIF-9(NH_2) clearly confirmed that the most intensive peaks belong to ZIF-9(NH_2) and the structure retained upon PTA impregnation. Moreover, the FT-IR spectrum of

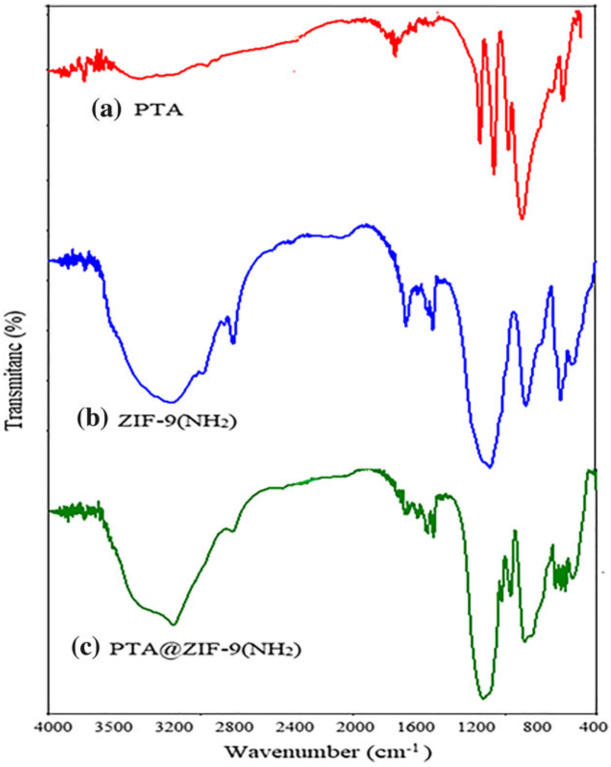

FIGURE 2 FT-IR spectra of (a) PTA, (b) ZIF-9(NH_2), (c) PTA@ZIF-9(NH_2)

PTA@ZIF-9(NH_2) exhibited the principal stretching modes of the Keggin PTA units at 1029, 952, 877 and 761 cm^{-1}, respectively. These bands correspond to the ν(P-O_a), terminal ν(W-O_t), corner-sharing ν(W-O_b) and edge-sharing ν(W-O_c) band vibrations of PTA, respectively.[42,43]

3.1.2 | X- ray diffraction and EDX

In the structure of ZIF-9(NH_2), four nitrogen atoms of four different benzimidazolate (bIm) ligands are coordinated to the cobalt (II) ion and each bIm ligand bridges two Co^{2+} ions and formed a sodalite topology framework.[44] The cobalt loading of 4.13 mmol.g^{-1} was found by elemental analysis with AAS for the ZIF-9(NH_2) which is close to the amount obtained for ZIF-9.[27] According to these structural information, XRD patterns of bare ZIF-9(NH_2) and PTA@ZIF-9(NH_2) were investigated (Figure 3). XRD patterns of the synthesized ZIF-9(NH_2) and PTA@ZIF-9(NH_2) were in good agreement with the reported XRD of ZIF-9.[27,45–47] The two sharp peaks at $2\theta < 10°$ in the XRD of bare ZIF-9(NH_2), demonstrated that a highly crystalline material was obtained. Moreover, the crystal structure of PTA@ZIF-9(NH_2) seems to remain unchanged during PTA grafting, while the intensity of some peaks were changed after the PTA impregnation. Broadening of some diffractions would be due to homogeneous dispersion of PTA on the surface of ZIF. However, a slight shift in some peak positions would be explained based on the dispersion of PTA over the surface of ZIF-9 and considerable interaction of PTA with the surface of ZIF-9 which may induce partial changes in the crystal structure of ZIF-9.[45] Observation of no diffraction peak for PTA in Figure 3b confirmed that the PTA was highly dispersed on ZIF-9(NH_2).[48] The energy dispersive X-ray (EDX) analysis of ZIF-9(NH_2) showed the main elements of Co, N, and C (Figure S1).

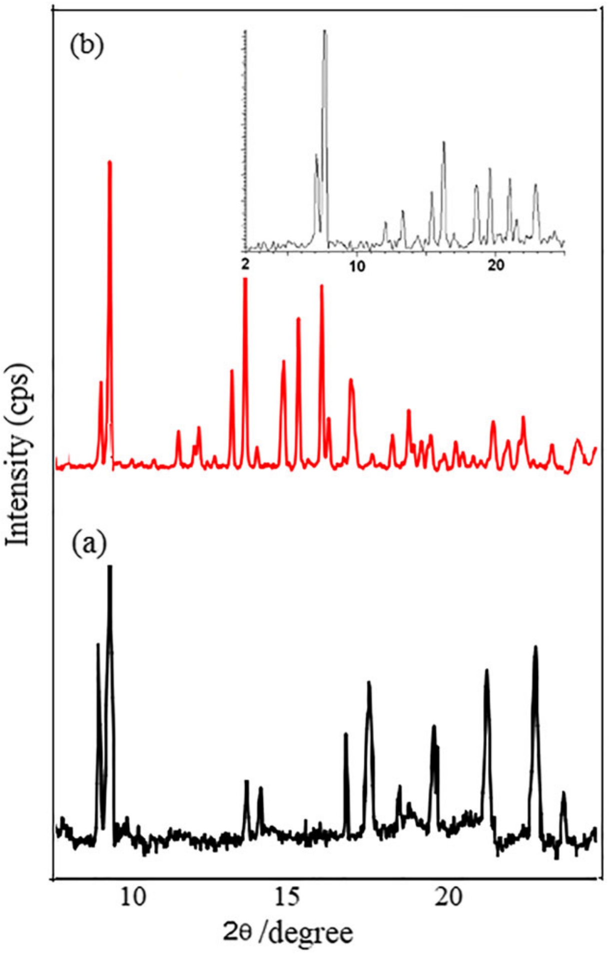

FIGURE 3 XRD patterns for ZIF-9(NH_2) (a) and PTA@ZIF-9(NH_2) (b). Inset shows XRD of the reported ZIF-9[27]

3.1.3 | TEM and SEM studies

Morphologies of the synthesized ZIF's were also studied. SEM and TEM micrographs of ZIF-9(NH_2) and SEM picture of PTA@ZIF-9(NH_2) are described in Figure 4, respectively. ZIF-9 showed uniform nanoparticles of

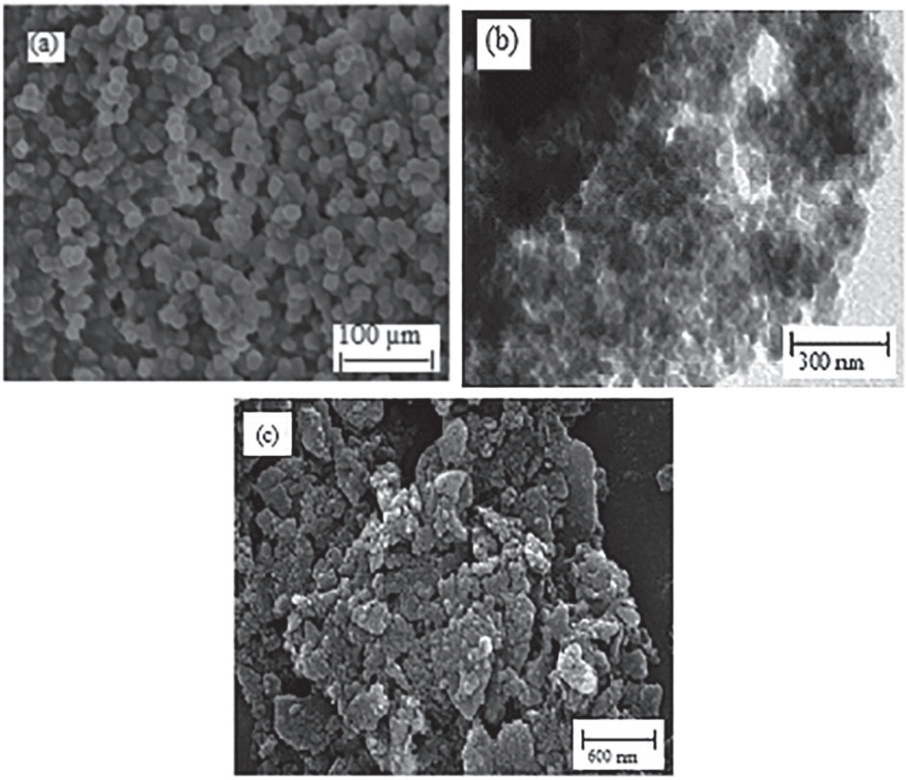

FIGURE 4 Electron microscopy of ZIF-9(NH_2) and PTA@ ZIF-9(NH_2). (a) SEM and (b) TEM micrographs of ZIF-9(NH_2), (c) SEM image of PTA@ ZIF-9(NH_2)

about 100 nm in size; but, PTA@ZIF-9(NH_2) indicated a disordered structure.[49] However, previous reports on ZIF-9 recommended that the pores are complex and may involve both micropore and mesopore arrays.[27] Moreover, grafting of PTA into the cage of ZIF may induce some demolition of ZIF-9 crystal structure and particles aggregation as shown in Figure 4b.[45]

3.1.4 | BET and TGA analysis of ZIF-9 (NH_2)

The nitrogen adsorption–desorption isotherms of ZIF-9(NH_2) sample measured at 77 K is shown in Figure S2. The type IV isotherm for ZIF-9(NH_2) along with a hysteresis loop at $P/P_0 = 0.85$–1 with an abrupt increase of gas adsorption at the mentioned relative pressures denoted the mesopores and macropores of the material.[50] The specific surface area of ZIF-9(NH_2) calculated by the BET method was 407 $m^2.g^{-1}$.[51,52] The BET surface area was substantially decreased upon the inclusion of PTA species (342 $m^2.g^{-1}$), which may indicate the presence of guest components supported on the ZIF-9(NH_2) framework. Furthermore, TGA analysis of ZIF-9(NH_2) confirmed an intended trend which was previously observed for ZIF-9 (Figure S3).[27] The weight loss at 150–220 °C is due to the removal of the adsorbed water and organic solvents; whereas the main weight loss at >550 °C corresponded to the combustion of the organic parts and destruction of the heteropolyacid moiety.

3.2 | *Catalytic performance of PTA@*ZIF-9(NH_2)

3.2.1 | Studying effect of the catalyst amount on the condensation reaction

The catalytic efficiency of PTA@ZIF-9(NH_2) heterogeneous catalytic system was assessed for the synthesis of ethyl-6-methyl-2-oxo-4-phenyl-1,2,3,4-tetrahydropyrimidine-5-carboxylate with various catalyst amounts (Figure 5). First, a model reaction was planned in the absence of catalyst. The reaction of benzaldehyde, ethyl acetoacetate and urea afforded 25% of the desired dihydropyrimidinone in the absence of catalyst after 30 min; whereas, 10 mg of catalyst afforded 65% of conversion at the same time. This finding revealed that the heterogeneous catalyst exhibited high catalytic activity in the desired transformation. Findings showed that 30 mg of catalyst was enough to endorse the reaction to 85% yield at a short time of 30 min. Higher amount of

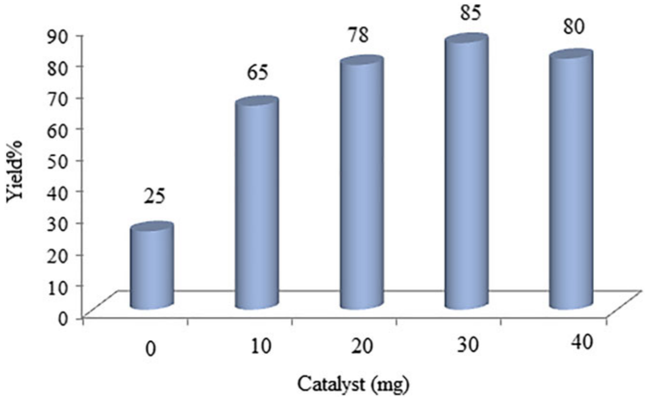

FIGURE 5 Effect of PTA@ZIF-9(NH_2) amount on the condensation of benzaldehyde (1 mmol), ethyl acetoacetate (1.2 mmol), and urea (1.5 mmol) at 110 °C after 30 min

catalyst, >30 mg, resulted in diminishing yield to 80% at the same time. This behavior would be explained considering the fact that increasing the number of active sites with enhancing catalyst amount, results decreasing concentration of reactants at the active sites, which leads to decline in yield%. Moreover, masses of catalyst >30 mg actually led to diffusion limited condition and no improvement in the yield% was attained.

3.2.2 | Catalytic efficacies of the ingredients

Condensation of benzaldehyde, ethyl acetoacetate and urea obtained only 12% of the desired product in the absence of catalyst after 30 min; whereas, 30 mg of $H_3PW_{12}O_{40}$ provided 35% yield after the same time (Table 1). Interestingly, ZIF-9(NH_2) was effective and 30 mg of it led to 32% yield after 30 min. The best yield was obtained with main catalyst PTA@ZIF-9(NH_2) and 85% yield attained after 30 min. Ionic grafting of HPA onto ZIF-9(NH_2) increased the dispersion of the catalytically active Brønsted acid sites throughout the network of ZIF-9(NH_2) and hence the best catalytic activity was observed.

TABLE 1 Catalytic activity of the ingredients in the preparation of 3,4-dihydropyrimidinones

Catalyst	Mass (mg)	Reaction time (min)	Yield%
-	-	30	12
$H_3PW_{12}O_{40}$	30	30	35
ZIF-9(NH_2)	30	30	32
PTA@ZIF-9(NH_2)	30	30	85

3.2.3 | Effect of reaction temperature on the condensation reaction

To enhance the yield% and accomplishing the best reaction conditions, the impact of temperature was contemplated on the condensation reaction of ethyl acetoacetate with benzaldehyde and urea in the presence of ZIF-9(NH_2), $H_3PW_{12}O_{40}$ and PTA@ZIF-9(NH_2) (Figure 6). As is anticipated, yield% was enhanced with temperature for all the examined catalysts and 32, 35, and 85% yields were obtained for ZIF-9(NH_2), $H_3PW_{12}O_{40}$ and PTA@ZIF-9(NH_2) at 110 °C after 30 min, respectively. Clearly, the principal catalyst PTA@ZIF-9(NH_2) acquired the best catalytic activity among the three inspected ingredients. Although, better yield (95%) was attained at 130 °C for PTA@ZIF-9(NH_2); however, considering the experimental requirements under scale-up conditions, the lower temperature 110 °C seems to be more suitable and accessible for large scale points of view. Consequently, the reaction temperature 110 °C was kept for all runs.

3.2.4 | Synthesis of different 3,4-dihydropyrimidin-2(1H)-ones

Under the optimized reaction condition, generality of the method was assessed by using different substituted aromatic aldehydes including electron withdrawing/releasing substituents on the phenyl ring in the presence of 10 mg PTA@ ZIF-9(NH_2) (Table 2). In accordance with past reports, aromatic aldehydes bearing electron releasing groups behaved better than those involving electron withdrawing ones. According to the reaction pathways introduced by several research groups,[53] the first step

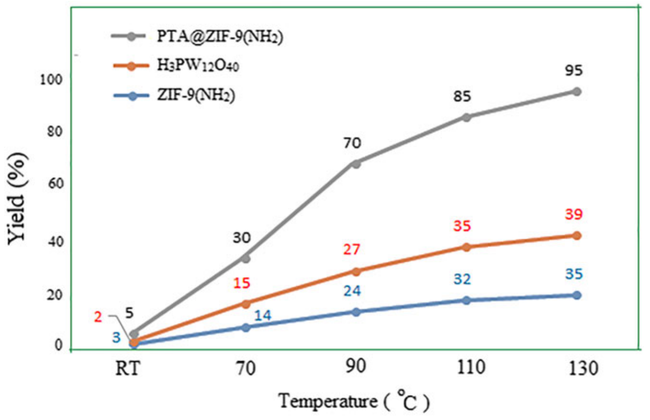

FIGURE 6 Effect of reaction temperature on the condensation of benzaldehyde (1 mmol), ethyl acetoacetate (1.2 mmol), and urea (1.5 mmol) in the presence of 0.03 g of PTA@ZIF-9(NH_2) after 30 min

TABLE 2 Three-component solventless condensation of ethyl acetoacetate, urea and different aldehydes catalyzed by PTA@ZIF-9(NH_2)

Entry	Aldehyde	product	Yield (%)	m.p.(°C)
1	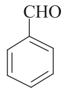	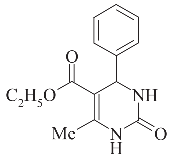	85	201–203
2	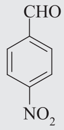	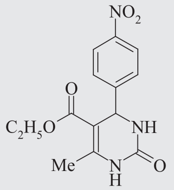	48	203–204
3	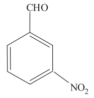	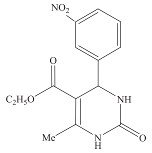	31	227–228
4	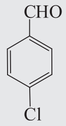	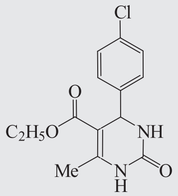	64	208–210
5	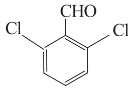	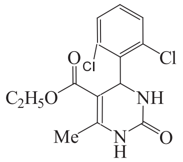	58	219–221
6	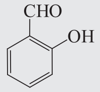	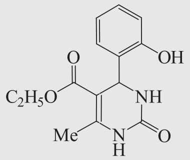	49	203–205
7	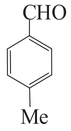	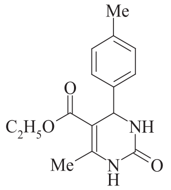	91	209–211
8	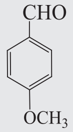	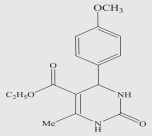	55	221–220

Reaction conditions: aldehyde (1 mmol), ethyl acetoacetate (1.2 mmol), urea (1.5 mmol). Reaction temperature and time 110 °C, 30 min. 30 mg of PTA@ZIF-9(NH_2) was used. Yields refer to the isolated 3,4-dihydropyrimidinone and probable side products. Selectivity wasn't considered.

of the mechanism involves formation of an acylimine intermediate by the reaction of the aromatic aldehyde with urea. Then, the iminium ion intermediate interacts with ethyl acetoacetate to produce an open chain ureide that subsequently cyclizes to the dihydropyrimidinone. It seems that electron releasing group on the phenyl ring of aromatic aldehyde, facilitates formation of this intermediate. Therefore, higher yields are obtained with aromatic aldehydes bearing electron releasing groups on phenyl rings.

3.2.5 | Comparing excellence of PTA@ZIF-9(NH_2) with some reported catalysts

Predominance of the present protocol was compared over some reported ones by observing the obtained yields (Table 3). The three component condensation of urea, acetoacetate, and benzaldehyde to prepare ethyl-6-methyl-4-(phenyl)-2-oxo-1,2,3,4-tetrahydropyrimidine-5-carboxylate was selected as a model reaction and the comparison was in terms of mol% of catalysts, reaction time, and percentage yield. Although, some of the reported additives led to marginally higher conversions, however, they required longer reaction times and higher mol% of catalyst. The present methodology used low

TABLE 3 Comparison of the reactivity of PTA@ ZIF-9(NH_2) with some other catalysts used for the synthesis of ethyl-6-methyl-4-(phenyl)-2-oxo-1,2,3,4-tetrahydropyrimidine-5-carboxylate

Catalyst	Catalyst amount	Time (h)	Yield (%)	Reaction cond.	Ref.
Si-[SbSipim] [PF_6]	0.4 g	3.5	90	Reflux in EtOH	[57]
Silica/PPA	0.3 g	0.5	85	Reflux in MeCN	[58]
Yb ($PFO)_3$	5 mol%	4	87	S. F., 120 °C	[59]
p-SA/ calixarene	0.5 mol%	8	81	Reflux in EtOH	[60]
HPA/Pip-SBA-15	0.6 g	0.3	90	100 °C	[38]
$NH_4H_2PO_4$/ MCM-41	0.04 g	6	72	S. F., 100 °C	[61]
Clay/HPA	0.05 mol%	1.5	87	S. F., 120 °C	[62]
[PEG-DAIL] [Cl]	0.3 mmol	5	86	Toluene, 80 °C	[54]
ZnO@SBA-15	0.02 g	2.5	96	EtOH, 65 °C	[63]
PTA@ZIF-9(NH_2)	0.01 g	0.5	86	110 °C	-

S. F refers to Solvent free.

catalyst amount under solvent-free condition and required relatively short reaction time.

3.2.6 | *Reusability of PTA@ZIF-9(NH$_2$)*

The ease of separation and reusability of a heterogeneous catalyst is an important issue which must be assessed during utilization of the catalyst. Consequently, PTA@ZIF-9(NH$_2$) nanocatalyst was probed for the recoverability and reusability in the Biginelli reaction over five consecutive runs. The condensation reaction was carried out with ethyl acetoacetate (1.2 mmol), benzaldehyde (1 mmol) and urea (1.5 mmol) at 110 °C under solvent-free condition in the presence of PTA@ ZIF-9(NH$_2$) (30 mg) for 30 min. Then, the catalyst was separated from the organic phase after the reaction and washed with abundant amounts of ethanol to get rid of any physisorbed reagents, and dried at room temperature for 6 hr after each run. Then, the recovered catalyst was reused under same reaction condition to those of the first run, and it was observed that PTA@ZIF-9(NH$_2$) nanocatalyst could be recovered easily and reused with a gradual decrease in activity (Figure 7). Comparison of the infrared spectra of PTA@ZIF-9(NH$_2$) before and after condensation reaction (regenerated after 5 runs) and observation of the characteristic bands around 800–1100 cm^{-1} clearly confirmed preservation of the *Keggin* structure.

3.3 | Hot filtration test

In order to find weather leaching of PTA occurred during the condensation reaction, a hot filtration test was planned. This experiment was accomplished to assess contribution of the leached active species into the reaction medium. Therefore, to a mixture of benzaldehyde (1 mmol), ethyl acetoacetate (1.2 mmol) and urea (1.5 mmol), 0.01 g of PTA@ZIF-9(NH$_2$) was added and the reaction was started for 15 min. At this stage, the yield of the product was 50%. At that point, hot chloroform was added and the catalyst was separated off and with the filtrate, the reaction was proceed for another 15 min at 100 °C. Yield% was enhanced to 58%; consequently, no significant increase in yield% was observed. This observation clearly affirmed the satisfactory steadiness of PTA@ZIF-9(NH$_2$) in the condensation reaction and no significant degradation of the catalyst occurred during the course of the reaction. ICP Analysis of the filtrate after separation of the catalyst proved that the grafted PTA was decreased from 18.8% in the fresh PTA@ZIF-9(NH$_2$) to 16.5% in the hot filtered catalyst. Therefore, 2.3% of the grafted PTA was leached from ZIF-9 during hot filtration test. These results were further asserted by the reproducibility and reusability investigations of the catalyst as specified previously.

3.4 | Some mechanistic highlights

According to the literature, condensation of benzaldehyde, ethyl acetoacetate and urea in the presence of PTA@ZIF-9(NH$_2$) was assessed under three different pathes (Figure 8).[54] For path A, we found that the Knoevenagel condensation product of benzaldehyde and ethyl acetoacetate did not afford the final product in the presence of urea and in the absence of catalyst; whereas, 25% of dihydropyrimidinone was attained in the presence of PTA@ ZIF-9(NH$_2$) ZIF-9(NH$_2$) after 30 min. This finding showed that the nanocatalyst revealed some basic characteristic in the reaction medium. In the case of path C, no significant amount of the final product was observed after 3 hr due to the low amount of the produced enaminone intermediate.[55,56] This study clearly confirmed the results obtained by Kadam et al on the

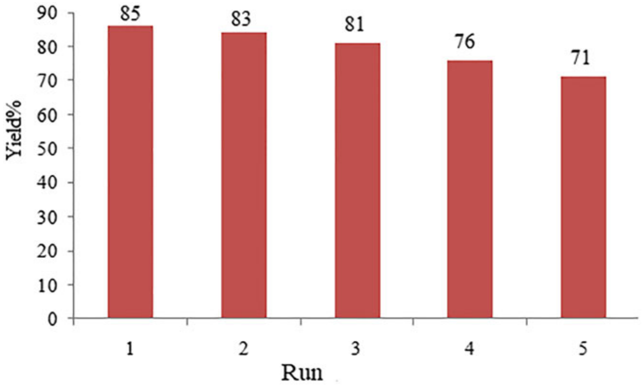

FIGURE 7 Yield% as a function of reusability of PTA@ZIF-9(NH$_2$) catalyst. Reaction temperature 100 °C. 30 mg of PTA@ ZIF-9(NH$_2$) was used and reaction time was 30 min

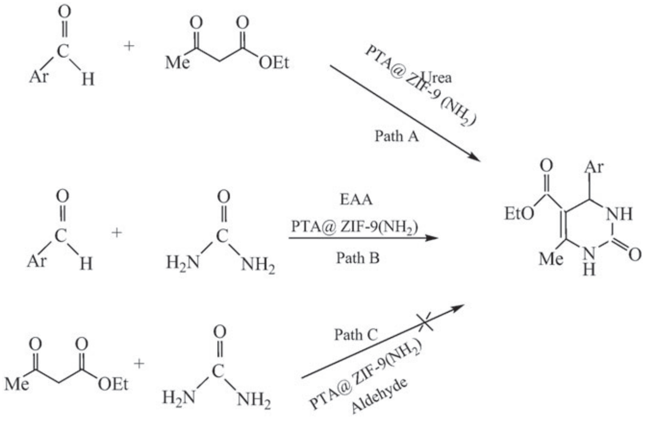

FIGURE 8 Suggested pathways for the synthesis of 3,4-dihydropyrimidin-2-(1H)-ones catalyzed by PTA@ ZIF-9(NH$_2$)

progress of the three-component condensation reaction through formation of the iminium ion (path B); furthermore, it was concluded that PTA@ZIF-9(NH_2) can show some basicity.

4 | CONCLUSIONS

In conclusion, PTA supported crystalline zeolitic imidazolate framework PTA@ ZIF-9(NH_2) was successfully synthesized and characterized using a variety of different techniques, including FT-IR, TEM, FESEM and XRD. Then, this new nanocatalyst was used as an efficient heterogeneous catalyst for the preparation of a range of 3,4-dihydropyrimidin-2-(1H)-ones. PTA@ZIF-9(NH_2) nanocatalyst could be reused several times without a significant decline in catalytic activity and no significant leaching of PTA was detected. It is apparent that PTA@ZIF-9(NH_2) nanocatalyst can be an alternative to other solid catalysts for the Bigineli condensation reaction. Interesting properties of PTA@ZIF-9(NH_2) such as non-toxic nature, easy to separate and recyclable material offer potential advantages over conventional catalysts, and would be suitable to the chemical industry.

ACKNOWLEDGEMENTS

This work has been supported by the Center for International Scientific Studies & Collaboration (CISSC). Partial financial/material support of Hakim Sabzevari university and Sabzevar university of medical sciences are greatly appreciated.

ORCID

Reza Tayebee https://orcid.org/0000-0003-1211-1472
Mehdi Baghayeri https://orcid.org/0000-0001-7438-9010
Behrooz Maleki https://orcid.org/0000-0002-3740-7096

REFERENCES

[1] H. K. Chae, D. Y. Siberio-Pérez, J. Kim, Y. Go, M. Eddaoudi, A. J. Matzger, M. O'keeffe, O. M. Yaghi, *Nature* **2004**, *427*, 523.

[2] D. J. Tranchemontagne, Z. Ni, M. O'Keeffe, O. M. Yaghi, *Angew. Chem. Int. Ed.* **2008**, *47*, 5136.

[3] S. S. Kaye, A. Dailly, O. M. Yaghi, J. R. Long, *J. Am. Chem. Soc.* **2007**, *129*, 14176.

[4] J. Lee, O. K. Farha, J. Roberts, K. A. Scheidt, S. T. Nguyen, J. T. Hupp, *Chem. Soc. Rev.* **2009**, *38*, 1450.

[5] A. Corma, H. García, F. X. Llabrés i Xamena, *Chem. Rev.* **2010**, *110*, 4606.

[6] S. Ma, H.-C. Zhou, *Chem. Commun.* **2010**, *46*, 44.

[7] Y. S. Li, F. Y. Liang, H. Bux, A. Feldhoff, W. S. Yang, J. Caro, *Angew. Chem. Int. Ed.* **2010**, *122*, 558.

[8] F. Nouar, J. Eckert, J. F. Eubank, P. Forster, M. Eddaoudi, *J. Am. Chem. Soc.* **2009**, *131*, 2864.

[9] P. Horcajada, T. Chalati, C. Serre, B. Gillet, C. Sebrie, T. Baati, J. F. Eubank, D. Heurtaux, P. Clayette, C. Kreuz, *Nat. Mater.* **2010**, *9*, 172.

[10] H. Li, M. Eddaoudi, M. O'Keeffe, O. M. Yaghi, *Nature* **1999**, *402*, 276.

[11] J. L. Rowsell, O. M. Yaghi, *Microporous Mesoporous Mater.* **2004**, *73*, 3.

[12] A. Phan, C. J. Doonan, F. J. Uribe-Romo, C. B. Knobler, M. O'keeffe, O. M. Yaghi, *Acc. Chem. Res.* **2010**, *43*, 58.

[13] S. R. Venna, M. A. Carreon, *J. Am. Chem. Soc.* **2009**, *132*, 76.

[14] S. Opelt, S. Türk, E. Dietzsch, A. Henschel, S. Kaskel, E. Klemm, *Cat. Com.* **2008**, *9*, 1286.

[15] Y. Zhou, J. Song, S. Liang, S. Hu, H. Liu, T. Jiang, B. Han, *J. Mol. Catal. A: Chem.* **2009**, *308*, 68.

[16] C. Chizallet, S. Lazare, D. Bazer-Bachi, F. Bonnier, V. Lecocq, E. Soyer, A.-A. Quoineaud, N. Bats, *J. Am. Chem. Soc.* **2010**, *132*, 12365.

[17] X. Liu, H. Li, L. P. Xiao, R. C. Sun, G. Song, *Green Chem.* **2019**, *21*, 1498.

[18] W. L. Xin, K. K. Lu, D. Shan, *Appl. Surf. Sci.* **2019**, *481*, 313.

[19] C. R. Li, J. Hai, L. Fan, S. L. Li, B. D. Wang, Z. Y. Yang, *Sens. Actuators B* **2019**, *284*, 213.

[20] D. Pan, S. Xu, Y. Miao, N. Xu, H. Wang, X. Song, L. Gao, G. Xiao, *Catal. Sci. Technol.* **2019**, *9*, 739.

[21] C. Song, X. Li, X. Zhu, S. Liu, F. Chen, F. Liu, L. Xu, *Appl. Catal. Gen.* **2016**, *5*, 48.

[22] F. Wang, M. X. Zhou, X. H. Yang, L. J. Gao, G. M. Xiao, *Mol. Catal.* **2017**, *432*, 144.

[23] J. Liu, J. He, L. Wang, R. Li, P. Chen, X. Rao, L. Deng, L. Rong, J. Lei, *Sci. Rep.* **2016**, *6*, 23667.

[24] M. Zhang, Q. Shang, Y. Wan, Q. Cheng, G. Liao, Z. Pan, *Appl. Catal. Environ.* **2019**, *241*, 149.

[25] J. Zakzeski, A. Dębczak, P. C. Bruijnincx, B. M. Weckhuysen, *Appl. Catal. Gen.* **2011**, *394*, 79.

[26] S. Bendt, M. Hovestadt, U. Böhme, C. Paula, M. Döpken, M. Hartmann, F. J. Keil, *Eur. J. Inorg. Chem.* **2016**, *2016*, 4440.

[27] L. T. Nguyen, K. K. Le, H. X. Truong, N. T. Phan, *Catal. Sci. Technol.* **2012**, *2*, 521.

[28] R. Tayebee, K. Savoji, M. K. Razi, B. Maleki, *RSC Adv.* **2016**, *6*, 55319.

[29] A. Hashemzadeh, M. M. Amini, R. Tayebee, A. Sadeghian, L. J. Durndell, M. A. Isaacs, A. Osatiashtiani, C. M. Parlett, A. F. Lee, *Mol. Catal.* **2017**, *440*, 96.

[30] N. M. Ghohe, R. Tayebee, M. M. Amini, A. Osatiashtiani, M. A. Isaacs, A. F. Lee, *Tetrahedron* **2017**, *73*, 5862.

[31] R. Tayebee, M. M. Amini, F. Nehzat, O. Sadeghi, M. Armaghan, *J. Mol. Catal. A: Chem.* **2013**, *366*, 140.

[32] R. Tayebee, M. Jarrahi, *RSC Adv.* **2015**, *5*, 21206.

[33] F. Hamy, V. Brondani, A. Flörsheimer, W. Stark, M. J. Blommers, T. Klimkait, *Biochemistry* **1998**, *37*, 5086.

[34] C. Santelli-Rouvier, B. Pradines, M. Berthelot, D. Parzy, J. Barbe, *Eur. J. Med. Chem.* **2004**, *39*, 735.

[35] M. J. Plunkett, J. A. Ellman, *Sci. Am.* **1997**, *276*, 68.

[36] C. Blackburn, B. Guan, J. Brown, C. Cullis, S. M. Condon, T. J. Jenkins, S. Peluso, Y. Ye, R. E. Gimeno, S. Punreddy, *Bioorg. Med. Chem. Lett.* **2006**, *16*, 3504.

[37] A. D. Patil, N. V. Kumar, W. C. Kokke, M. F. Bean, A. J. Freyer, C. D. Brosse, S. Mai, A. Truneh, B. Carte, *J. Org. Chem.* **1995**, *60*, 1182.

[38] R. Tayebee, M. M. Amini, M. Ghadamgahi, M. Armaghan, *J. Mol. Catal. A: Chem.* **2013**, *366*, 266.

[39] K. S. Park, Z. Ni, A. P. Côté, J. Y. Choi, R. Huang, F. J. Uribe-Romo, H. K. Chae, M. O'Keeffe, O. M. Yaghi, *Proc. Natl. Acad. Sci.* **2006**, *103*, 10186.

[40] B. Hachuła, M. Nowak, J. Kusz, *J. Chem. Crystallogr.* **2010**, *40*, 201.

[41] S. Mohan, N. Sundaraganesan, J. Mink, *Spectrochim. Acta, Part a* **1991**, *47*, 1111.

[42] J.-W. Liu, Y.-C. Liu, H. He, B.-F. Yang, G.-Y. Yang, *Inorg. Chem. Commun.* **2015**, *53*, 60.

[43] R. Li, X. Ren, J. Zhao, X. Feng, X. Jiang, X. Fan, Z. Lin, X. Li, C. Hu, B. Wang, *J. Mater. Chem. A* **2014**, *2*, 2168.

[44] D. Y. Lee, S. J. Yoon, N. K. Shrestha, S.-H. Lee, H. Ahn, S.-H. Han, *Microporous Mesoporous Mater.* **2012**, *153*, 163.

[45] A. Noguera-Díaz, J. Villarroel-Rocha, V. P. Ting, N. Bimbo, K. Sapag, T. J. Mays, *J. Chem. Technol. Biotechnol.* **2019**, *94*. https://doi.org/10.1002/jctb.5947

[46] Y. Li, X. Zhang, X. Chen, K. Tang, Q. Meng, C. Shen, G. Zhang, *ACS Appl. Mater. Interfaces* **2019**. https://doi.org/10.1021/acsami.9b00958

[47] Z. Ozturk, J. P. Hofmann, M. Lutz, M. Mazaj, N. Z. Logar, B. M. Weckhuysen, *Eur. J. Inorg. Chem.* **2015**, *2015*, 1625.

[48] L. Chen, B. Bai, *Int. J. Photoenergy* **2013**. https://doi.org/10.1155/2013/406158, *2013*, 1.

[49] M. He, J. Yao, Q. Liu, Z. Zhong, H. Wang, *Dalton Trans.* **2013**, *42*, 16608.

[50] A. Noguera-Díaz, J. Villarroel-Rocha, V. P. Ting, N. Bimbo, K. Sapag, T. J. Mays, *J. Chem. Technol. Biotechnol.* **2019**. https://doi.org/10.1002/jctb.5947

[51] W. Ren, J. Gao, C. Lei, Y. Xie, Y. Cai, Q. Ni, J. Yao, *Chem. Eng. J.* **2018**, *349*, 766.

[52] J. Dai, S. Xiao, J. Liu, J. He, J. Lei, L. Wang, *RSC Adv.* **2017**, *7*, 6288.

[53] R. Tayebee, B. Maleki, M. Ghadamgahi, *Chin. J. Catal.* **2012**, *33*, 659.

[54] N. D. Kadam, R. V. Jayaram, *Curr. Catal.* **2018**, *7*, 52.

[55] M. Rahman, A. Sarkar, M. Ghosh, A. Majee, A. Hajra, *Tetrahedron Lett.* **2014**, *55*, 235.

[56] Z.-L. Shen, X.-P. Xu, S.-J. Ji, *J. Org. Chem.* **2010**, *75*, 1162.

[57] L.-Q. Kang, D.-Y. Jin, Y.-Q. Cai, *Synth. Commun.* **2013**, *43*, 1896.

[58] M. Zeinali-Dastmalbaf, A. Davoodnia, M. M. Heravi, N. Tavakoli-Hoseini, A. Khojastehnezhad, H. A. Zamani, *Bull. Korean Chem. Soc.* **2011**, *32*, 656.

[59] M. Wu, J. Yu, W. Zhao, J. Wu, S. Cao, *J. Fluorine Chem.* **2011**, *132*, 155.

[60] D. L. Da Silva, S. A. Fernandes, A. A. Sabino, Â. de Fátima, *Tetrahedron Lett.* **2011**, *52*, 6328.

[61] R. Tayebee, M. Ghadamgahi, *Arab. J. Chem.* **2017**, *10*, 757.

[62] K. Selvakumar, T. Shanmugaprabha, M. Kumaresan, P. Sami, *Synth. Commun.* **2018**, *48*(2), 223.

[63] D. Bhuyan, M. Saikia, L. Saikia, *Microporous Mesoporous Mater.* **2018**, *256*, 39.

[64] S. Wang, W. Yao, J. Lin, Z. Ding, X. Wang, *Angew. Chem. Int. Ed.* **2014**, *53*, 1034.

SUPPORTING INFORMATION

Additional supporting information may be found online in the Supporting Information section at the end of the article.

How to cite this article: Tayebee R, Fattahi Abdizadeh M, Erfaninia N, et al. Phosphotungstic acid grafted zeolite imidazolate framework as an effective heterogeneous nanocatalyst for the one-pot solvent-free synthesis of 3,4-dihydropyrimidinones. *Appl Organometal Chem*. 2019;e4959. https://doi.org/10.1002/aoc.4959